NCAT Report 05-02

WHEEL WANDER AT THE NCAT TEST TRACK

By

David H. Timm
Angela L. Priest

April 2005

277 Technology Parkway Auburn, AL 36830

WHEEL WANDER AT THE NCAT TEST TRACK

By:

Dr. David H. Timm, P.E.
Gottlieb Assistant Professor of Civil Engineering
National Center for Asphalt Technology
Auburn University, Auburn, Alabama

Angela L. Priest
Graduate Research Assistant
National Center for Asphalt Technology
Auburn University, Auburn, Alabama

NCAT Report 05-02

April 2005

DISCLAIMER

The contents of this report reflect the views of the authors who are solely responsible for the facts and the accuracy of the data presented herein. The contents do not necessarily reflect the official view and policies of the National Center for Asphalt Technology of Auburn University. This report does not constitute a standard, specification, or regulation.

ACKNOWLEDGEMENTS

The authors wish to acknowledge the Alabama Department of Transportation, the Indiana Department of Transportation and the Federal Highway Administration for their support of the Structural Experiment at the Test Track. Also, many thanks to Buzz Powell, Scott Parker, Jennifer Still and Michael Newberry for their assistance and expertise in installing the lateral positioning system. Finally, Tom McEwen deserves special recognition for all his technical assistance.

TABLE OF CONTENTS

LIST OF FIGURES

WHEEL WANDER AT THE NCAT TEST TRACK

David H. Timm & Angela L. Priest

INTRODUCTION

Background

Wheel wander, or the lateral distribution of wheel loads, is a natural phenomenon observed on public-access roadways. Various vehicle types, individual driving habits, wind effects, mechanical alignment of trailers and other factors all contribute to the randomness of wheel tracking (Buiter et al., 1989). Further, Blab and Litzka (1995) identified lane width, vehicle speed, existing cross-sectional rut-depth and vehicle width as critical factors in the amount of wander. Figure 1 illustrates an example of a normally-distributed wheel wander pattern collected in Michigan, which is representative of many open-access facilities (Stempihar et al., 2005).

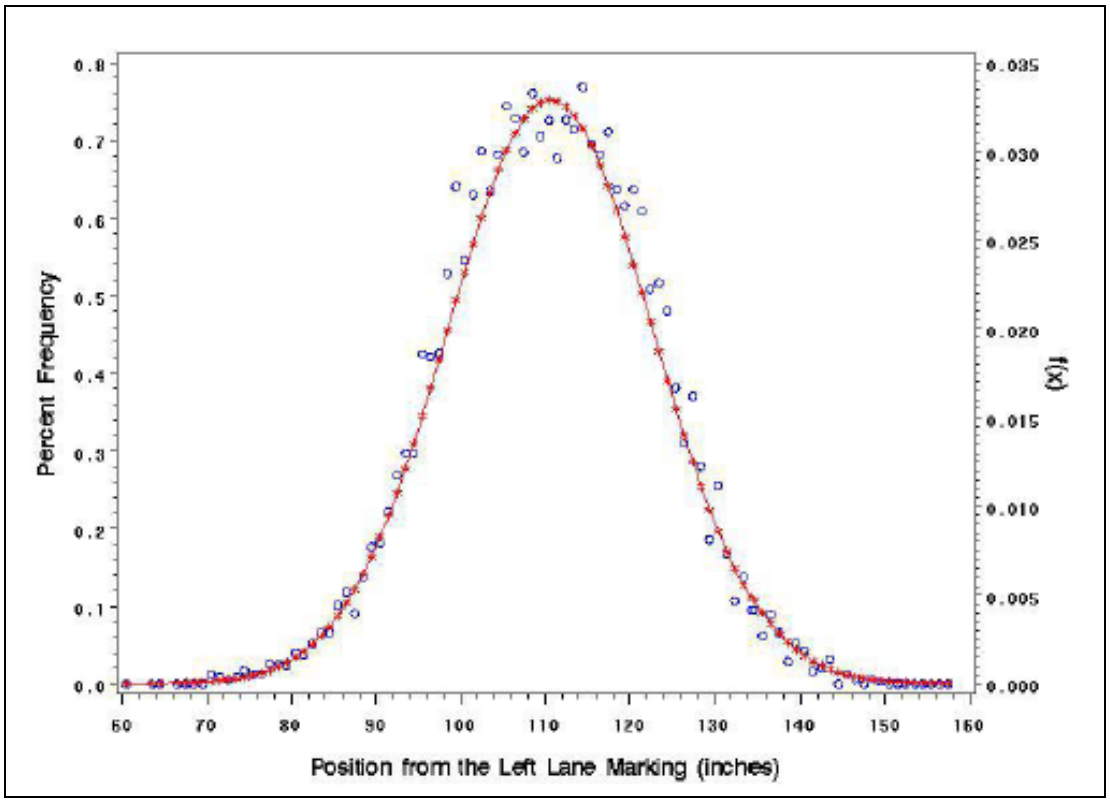

Figure 1. Measured Wheel Wander in Michigan (Stempihar et al., 2005).

From a pavement design and performance perspective, wheel wander is critical since it dictates where the loads are placed and the frequency with which a point in the pavement is loaded. Also, in the absence of wheel wander, pavement damage is much greater. This has been observed under heavy-vehicle simulators when wheel wander is removed. It was also observed at the WESTRACK experiment where robotically-driven trucks initially trafficked test sections with little or no wheel wander (Epps et al., 2002). In reality, wheel wander tends to be normally distributed with a standard deviation ranging from 8 to 24 in., as indicated by a number of field

studies (Buiter et al., 1989; Timm, 1996; Stempihar et al., 2005). The difference in standard deviation has been shown to depend primarily upon the route and the respective lane width (Buiter et al., 1989).

Wheel wander is an important issue pertaining to the validity of research underway at the National Center for Asphalt Technology (NCAT) Test Track. Since the Test Track is meant to simulate open-access facilities, it is imperative that realistic wheel wander patterns be applied during testing. A number of factors could lead to non-realistic wheel wander on the Test Track. First, the traffic consists of only two types of test vehicles (pictured in Figure 2), so the randomness of different vehicle types has been effectively reduced compared to open-access facilities. Second, the driver pool consists of ten drivers over two shifts per day further reducing the natural randomness found on open-access roads. Third, because the Test Track is a closed loop, shown in Figure 3, there is potential that the repetitive environment will cause the trucks to track consistently along the same line.

a) Triple Trailer

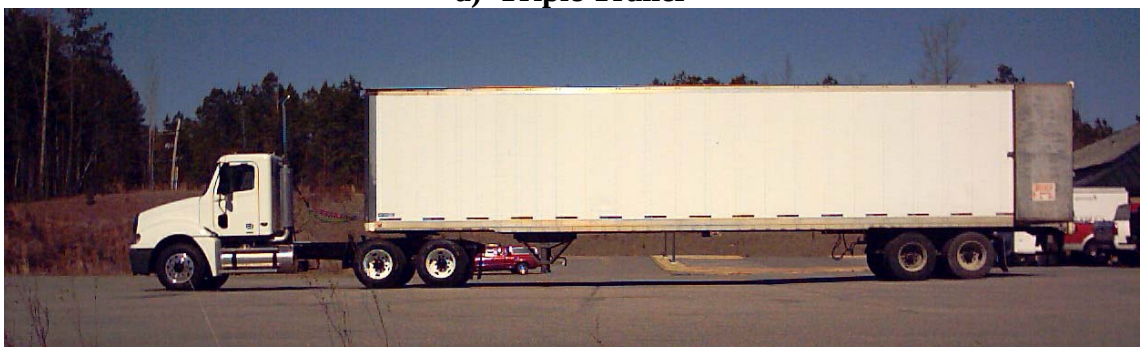

b) Box Trailer

Figure 2. NCAT Test Track Vehicles.

Figure 3. NCAT Test Track.

Another important consideration for the Test Track is determining the lateral placement of loads relative to the embedded instrumentation in sections N1 through N8. These test sections include gauges to measure strain and pressure under live traffic loading. Theoretically, the measured responses are a function of load placement; therefore it is necessary to measure where the loads are placed relative to the gauges. For example, Figure 4 depicts the theoretical relationship between the center of a tire load and the strain response at the bottom of the asphalt layer. The graph was generated using WESLEA for Windows, a linear layered elastic model for pavement response analysis. As indicated in the figure, a 6 kip load with 100 psi contact stress was simulated on a 7 in. HMA full depth pavement.

While the magnitude of the pavement response is certainly a function of the loading, pavement depth and properties, the shape of the curve in Figure 4 is representative of typical pavement sections. This relationship is further defined by fitting a second-order polynomial to the simulated data as shown in Figure 5. The form of this equation, in addition to a less-complex linear model, was used in this study when evaluating field-measured strain and distance data.

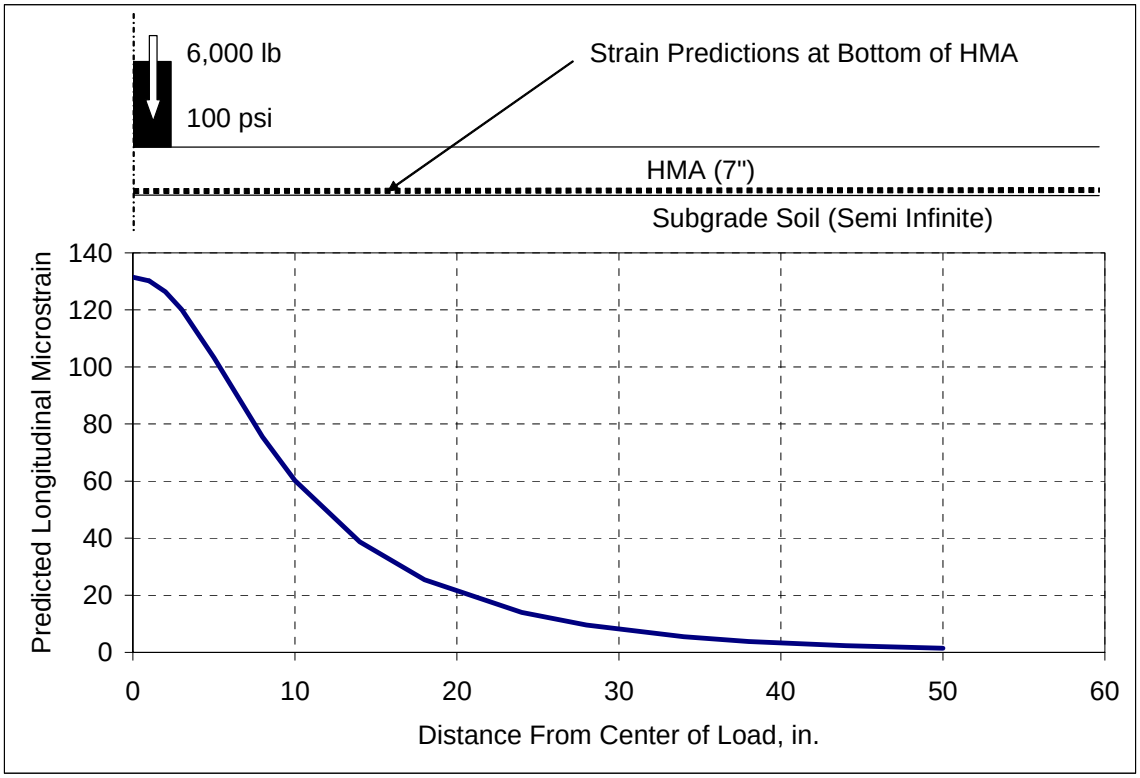

Figure 4. Theoretical Relationship Between Strain and Distance.

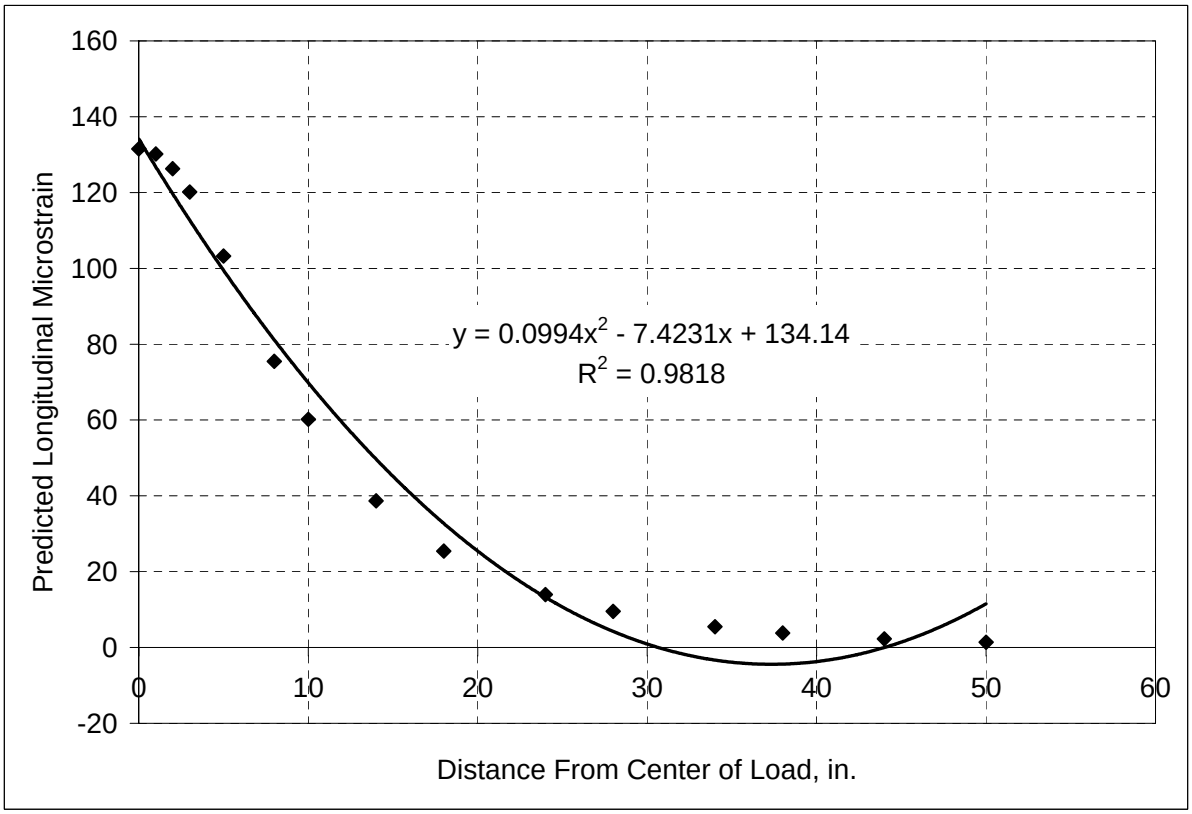

Figure 5. Statistical Fit to Theoretical Strain Predictions.

Objectives

To address the issues described above, the objectives of this study were:
1. Devise a means of accurately measuring the lateral placement of wheel loads.
2. Characterize the wheel wander pattern at the NCAT Test Track.
3. Assess the effect of wheel placement on measured pavement response.

Scope

A lateral positioning system, consisting of three axle-sensing strips, was assembled and installed at the NCAT Test Track. Calibration studies were conducted to verify the measurements, and five hours of live traffic data were collected and analyzed. This report documents the system, installation procedures, governing equations, calibration procedures, calibration results and results of the live testing.

LATERAL POSITIONING – GENERAL APPROACH

Though many approaches to measuring wheel wander are available, ranging from precision cameras to Global Positioning Systems (GPS), it was decided to implement a system similar to that used at the Minnesota Road Research Project (Mn/ROAD). The Mn/ROAD system consisted of three embedded axle sensing strips in a precise geometric arrangement that enabled the measurement of lateral wheel position. A similar system for the Test Track was relatively inexpensive (less than $2000, installed), was compatible with the existing data acquisition equipment in use at the Test Track and was shown to give accurate results at Mn/ROAD (Timm, 1996). Also, as will be discussed later, the system was relatively easy to install, calibrate and execute wheel wander studies.

The key to the lateral position system is the geometric arrangement of the axle sensing strips, shown schematically in Figure 6. In addition to the sensors and pavement markings, the figure indicates a particular wheel track, at a lateral offset of y′, and corresponding time stamps (t_1, t_2 and t_3) when each sensor records the passage of the wheel. The following derivation shows how the lateral position, y′, is determined from the time stamps and geometry of the sensor configuration using parameters defined in Figure 6.

1. Calculate the velocity, v, of the axle as it moves from the first to the third sensor by:
$$v = \frac{x}{t_3 - t_1} \tag{1}$$
2. Assuming that the velocity remains constant as the axle passes over the sensors, the following velocity relationship also holds true between the first and second sensor:
$$v = \frac{f + x'}{t_2 - t_1} \tag{2}$$
3. Equating equations (1) and (2) and solving for x′ yields:
$$x' = \frac{x}{t_3 - t_1} \cdot (t_2 - t_1) - f \tag{3}$$

4. Given the angle of orientation (α) of the second sensor, the following equation holds:

$$\tan\alpha = \frac{y'}{x'} \tag{4}$$

5. Substituting the expression for x′ in equation (3) and solving for y′ in equation (4) produces the desired result:

$$y' = (\tan\alpha)\cdot\left[\frac{x}{t_3 - t_1}\cdot(t_2 - t_1) - f\right] \tag{5}$$

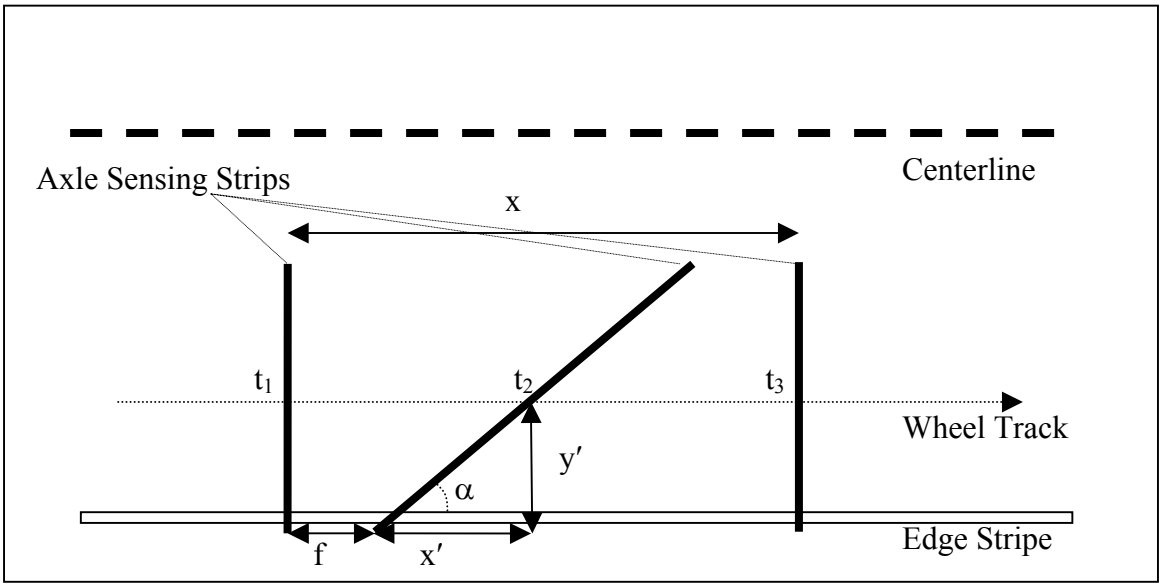

Figure 6. Lateral Positioning System – Plan View.

As observed through the equations presented above, precision was required during installation to ensure accurate wheel placement measurements. Also, the system required data acquisition capable of high sampling rates since trucks traveling at 45 mph results in only tenths of a second between time stamps. These issues are more fully discussed below.

AXLE SENSING EQUIPMENT AND INSTALLATION

The axle sensing strips shown schematically in Figure 6 were obtained from International Road Dynamics, Inc (IRD). Two models were obtained; the AS400 was used for the parallel sensors (1 and 3), while model AS405 (almost three feet longer) was used for the diagonal sensor (2). Additionally, each sensor was shipped with an installation kit and signal processing card.

Principle of Operation

The axle sensing strips are approximately 1 in. x 1 in. The AS400 sensors are 88 in. long while the AS405 sensor is 120 in. Both types are made of a resistive material sensitive to pressure and enclosed in a semi-rigid casing that is impervious to moisture. Under no-load conditions, the resistance of each sensor exceeds 10 MΩ. Upon application of pressure from a passing wheel, the resistance is dramatically reduced to between 2,000 Ω and 50,000 Ω. The goal is to measure with great precision the time at which the resistance changes to determine t_1, t_2 and t_3, as shown

in Figure 6.

Sensor Installation

Since only one set of axle sensing strips was procured, care was taken to select a location that was representative of the structural experiment (sections N1 through N8 as indicated in Figure 7). The transition zone between N3 and N4 was selected since it was the approximate midpoint of the test sections, was far enough from the east curve to be representative of the tangent sections and was in one of the two thickest sections which is most likely to not require rehabilitation (and thus removal of the lateral positioning sensors) before the end of the traffic cycle in 2005.

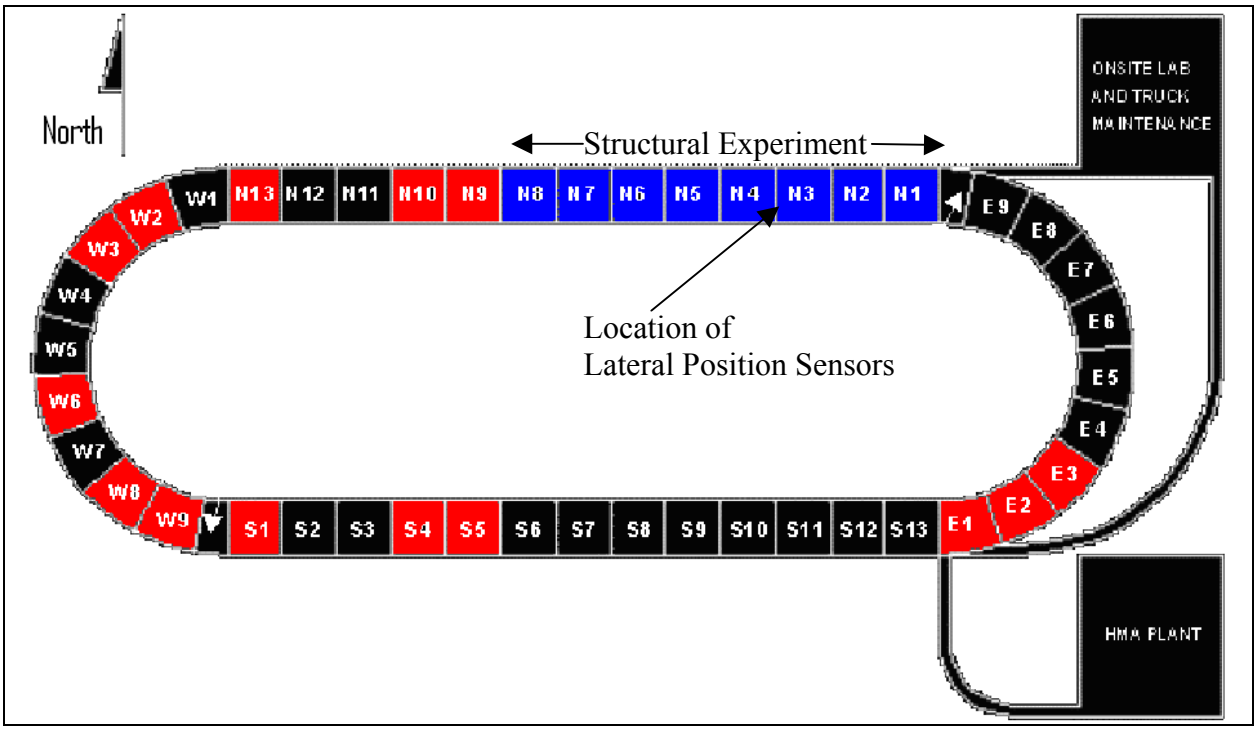

Figure 7. Test Track Layout and Sensor Location.

Figure 8 illustrates the precise geometric layout of the sensors installed in N4. In the figure, distances are given from the transverse joint between N3 and N4 to each sensor. The inside edge of the shoulder stripe was used to reference transverse distances. It was decided to extend the sensors a short distance into the shoulder area since visual observation of the trucks indicated that there was some tendency to drift over the edge stripe. Also, it was desirable to place the sensors to predominantly measure the outside half of each axle, rather than get "double-hits" from the inside half of an axle hitting the upper portion of the diagonal sensor. Eliminating "double-hits" greatly simplified data processing, as will be discussed later.

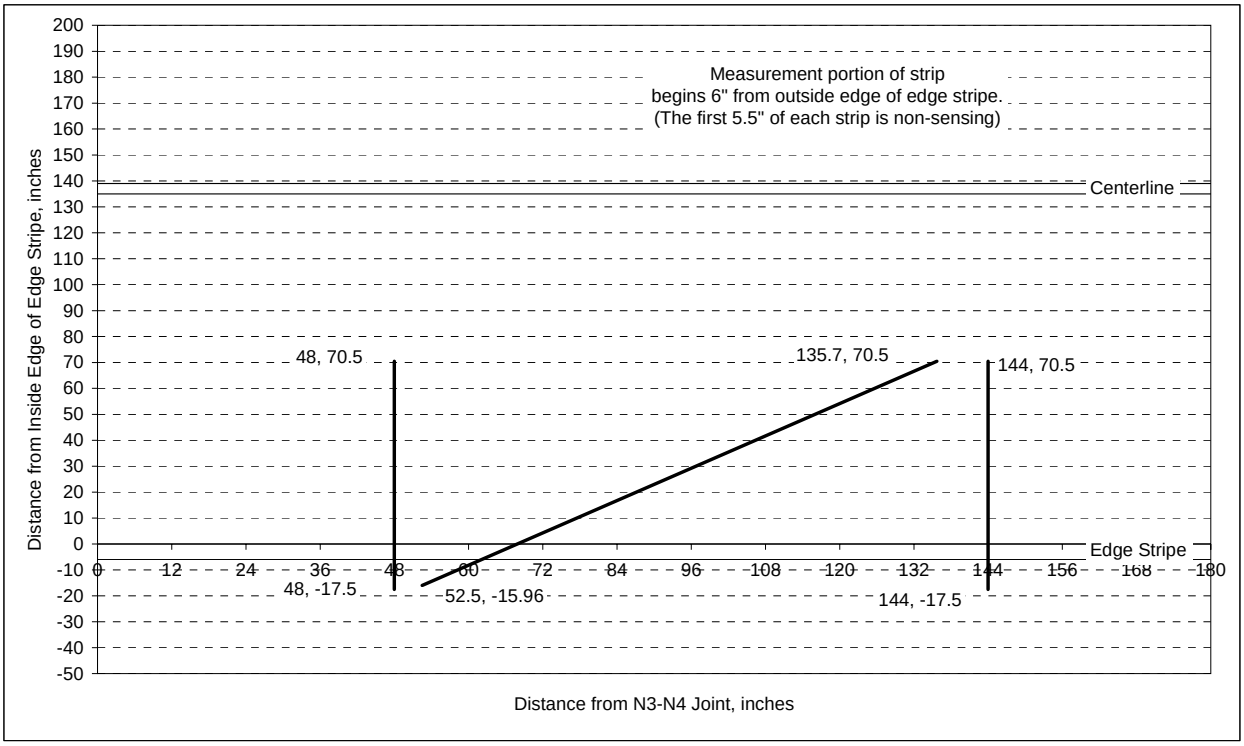

Figure 8. Lateral Positioning System Layout.

While only highlights of the installation process are provided here, detailed instructions regarding sensor installation can be found in the IRD installation manual (IRD, 2003). The first step, illustrated in Figure 9, was to layout string lines and mark the gauge locations on the pavement according to the dimensions given in Figure 8.

Figure 9. Laying Out Sensor Locations.

After the gauge locations had been marked and verified, a concrete saw was used to cut slots in the pavement approximately 1.5 in. wide by 1.5 in. deep as illustrated in Figure 10. A hammer drill was used to chip out each slot to make a trough for the sensor as pictured in Figure 11. Throughout this process, the depth was checked to ensure the proper slot size. A leaf blower was then used to dry out the slots and remove the debris from around the gauge locations (Figure 12). This helped speed drying time and minimized the total installation time. Once the slots were

clean and ready for installation, metal brackets supplied by IRD were attached to each sensor to suspend each sensor as shown schematically in Figure 13.

Figure 10. Cutting Sensor Slots.

Figure 11. Chipping Out the Sensor Slots.

Figure 12. Cleaning Sensor Slots.

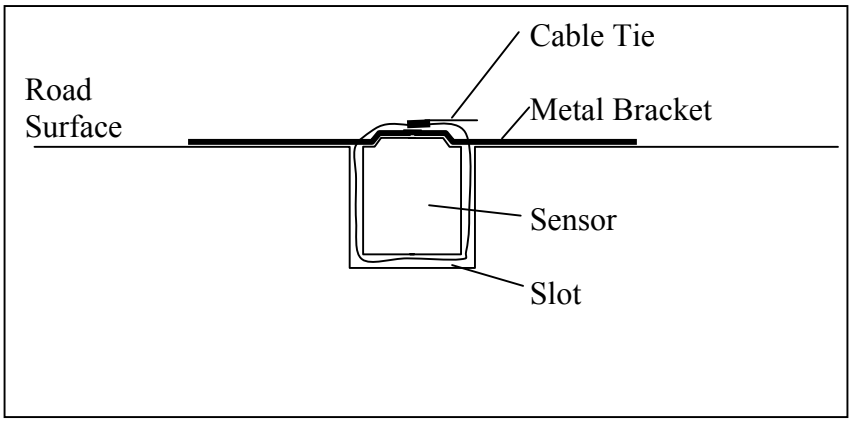

Figure 13. Checking Slot Depth Before Installation.

An epoxy, also supplied by IRD, Inc., was mixed with grout using a mechanical mixer and placed in each of the sensor slots. Duct tape, that was later removed to give a "clean" final installation, was placed along the edge of each slot prior to installation. The sensors were then placed in each slot and gently worked back and forth to eliminate any air bubbles between the sensor and grout/epoxy mixture. It was important to remove any excess grout/epoxy from the surface of the gauges since it could affect sensor readings. This was done with hand tools and shop rags. Surplus asphalt pills were used as weights on the metal brackets to hold the sensors in place while the epoxy cured. These steps are highlighted in Figure 14.

After the epoxy had solidified, the weights were removed from the brackets. The cable ties attaching each bracket were cut and the brackets and duct tape were removed as well. The final installation is pictured in Figure 15.

a) Mixing Epoxy

b) Placing Sensor

c) Sensor In-place, Waiting for Cure Time

Figure 14. Final Placement of Sensors.

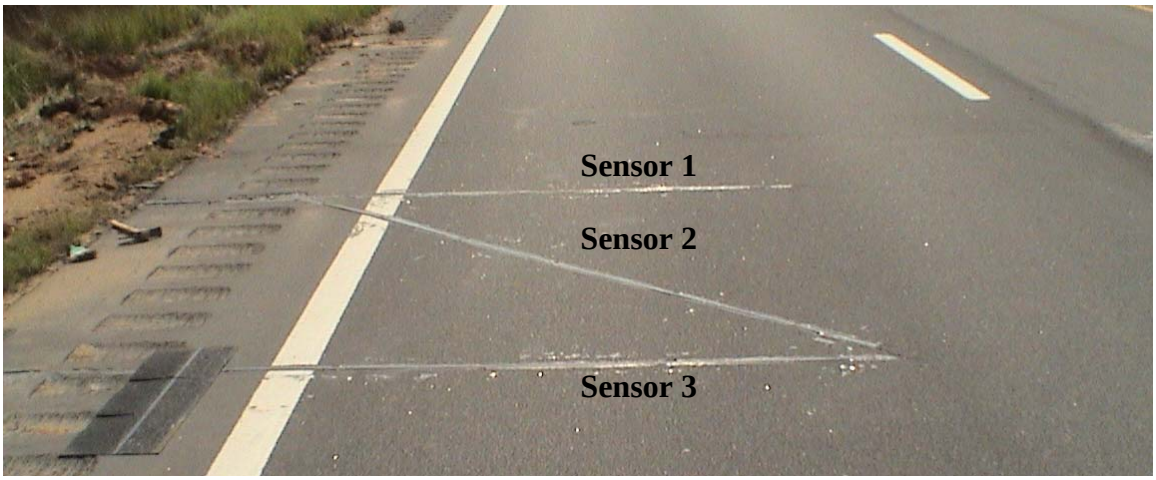

Figure 15. Final Installation.

The remaining work consisted of connecting the lead wires to the roadside data acquisition box. Buried conduit was used to protect the cables as pictured in Figure 16. The roadside data acquisition box consisted of a Campbell-Scientific battery pack charged from a solar panel and a signal processing card supplied by IRD (called a "Treadle" card) as pictured in Figure 17. The roadside box is not capable of storing any data and requires an external collection and storage system. Therefore, the portable Dataq data acquisition system and accompanying laptop computer, also used for the other data collection in the structural experiment (Timm et al., 2004), was used to collect and store data when conducting lateral positioning studies.

Figure 16. Burying Cable From Sensors to Data Acquisition Box.

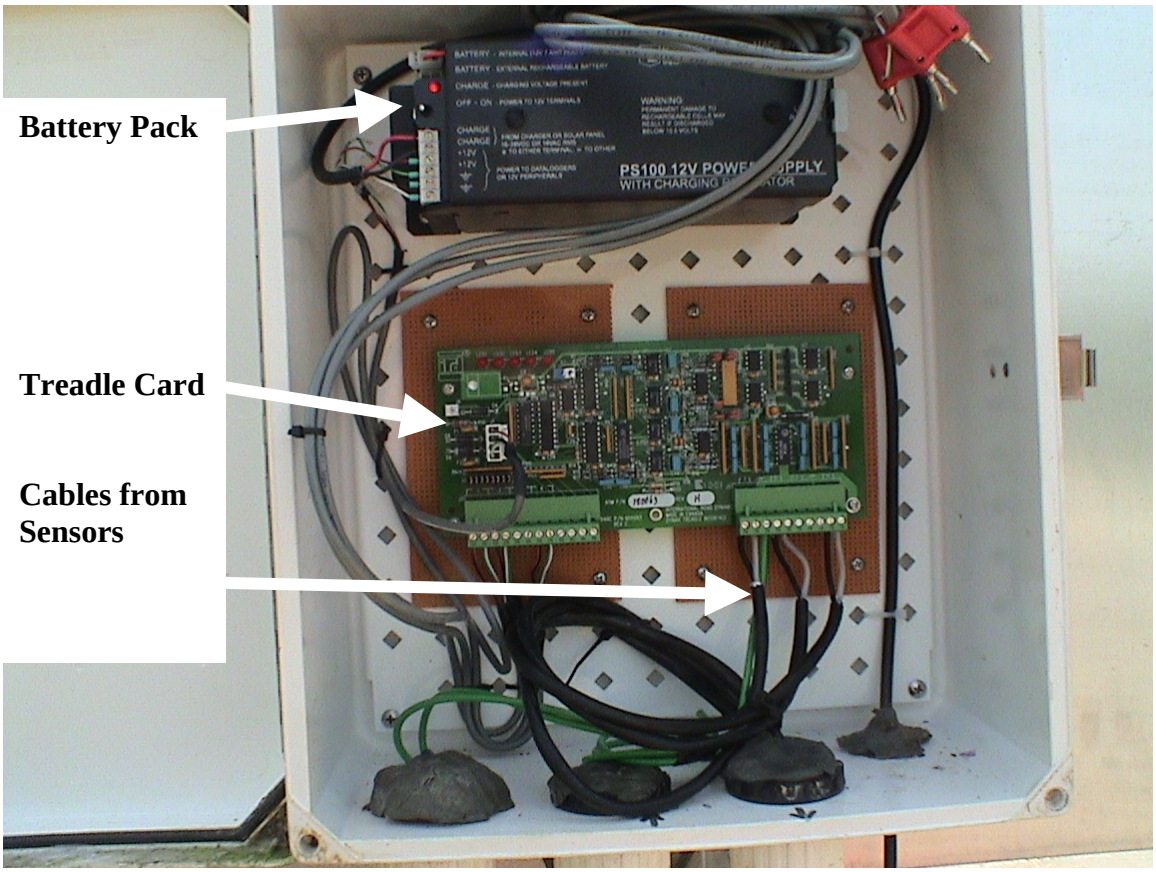

Figure 17. Data Acquisition Box.

DATA ACQUISITION AND SIGNAL PROCESSING

When conducting lateral positioning studies, a high sampling rate is essential to accurately measure exactly when each strip senses an axle. For this study, the Dataq system was operated in "triggered" mode and sampled at 2,000 Hz. For each truck pass, a triggered burst of data was recorded to capture each axle of each truck. Under this scheme, the precision of t_1, t_2 and t_3 was to the microsecond. Figure 18 illustrates typical sensor readings for the passage of one triple-trailer truck. The three traces correspond to each sensor and it is evident when the axle is passing over the gauge from the reduction in voltage (the Treadle card converts the resistance change in the sensor into a voltage change to facilitate measurement). The time stamps (t_1, t_2 and t_3) are taken as the first point below the no-load reading and the individual axle readings are clearly evident as indicated by the notation in the "Sensor 1" window of Figure 18.

Figure 18. Dataq Recording of One Truck Pass.

Since the traces, as shown in Figure 18, were relatively stable, no additional cleaning of the signal was required. A unique algorithm to determine the time stamps was developed specifically for this research and implemented in a commercially-available engineering spreadsheet called DaDisp. The algorithm examines each trace and finds the first point below the baseline (no-load) reading for each axle pass. The full algorithm is given in Appendix A. Equation 5, presented above, is then used with the geometric data to determine the lateral offset for each passage of each axle.

SYSTEM CALIBRATION

As a check of the installation, data collection and calculation procedures, the system required a simple calibration test. To accomplish this task, five readings were taken with a passenger car. A line of fine sand was placed parallel to and just past the third sensor so that the offset distance could be physically measured by the marks in the sand. These measurements were then compared to the computed offset, and the results are presented in Figure 19. It was concluded that the system is very accurate and is a nearly perfect representation of the physical measurements. It should also be noted that the distances were measured to the center of the tire.

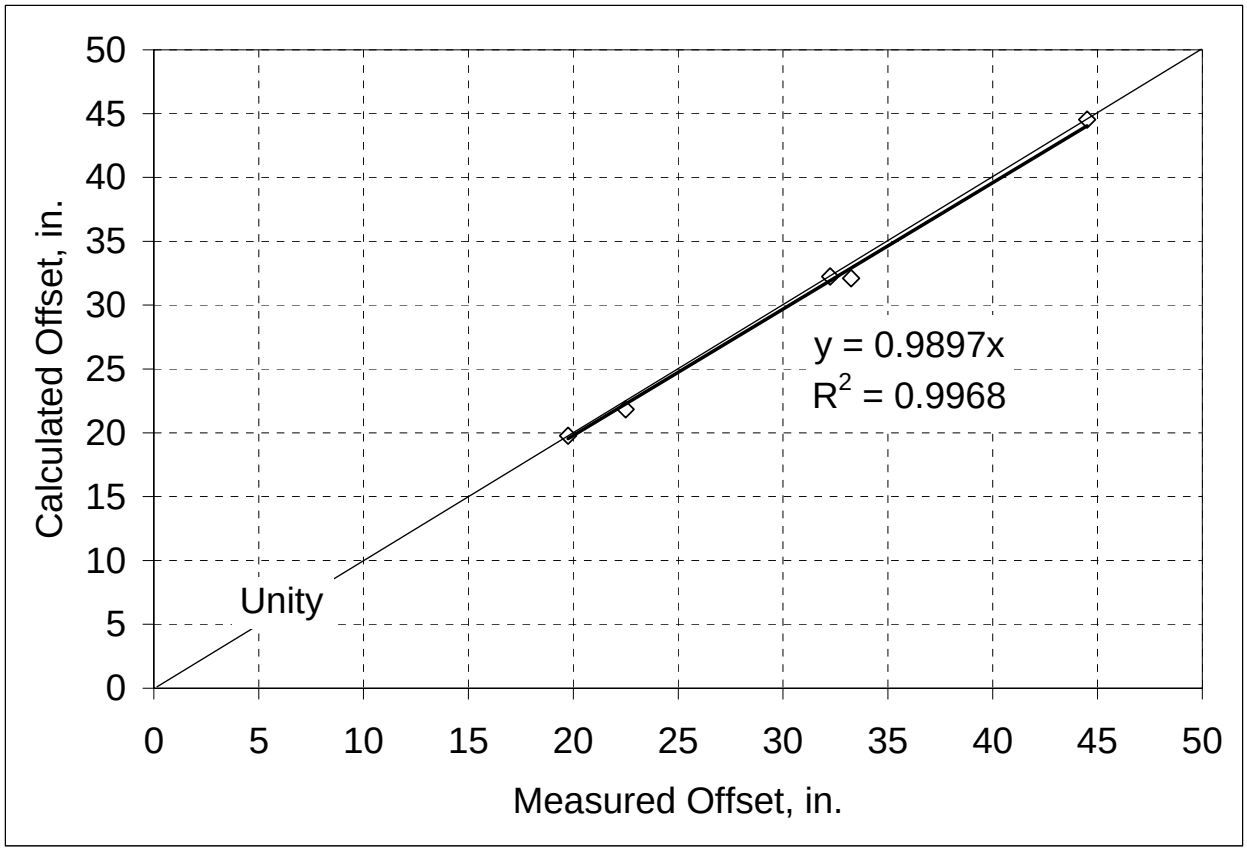

Figure 19. Lateral Positioning System Calibration Data.

WHEEL WANDER STUDIES

After the system had been installed, checked and calibrated, data were collected over a 2.5 hour period from both a morning and afternoon shift on July 21, 2004. The data were examined from a number of perspectives. First, all axles were considered together to determine the overall wheel wander pattern. Second, the axles were identified separately by their order on each of the individual vehicles (i.e, steer axle, second axle, third axle, etc.). Finally, an analysis was done examining the relationship between the wheel wander and measured strain responses.

Wheel Wander of All Axles

Histograms were generated from the wheel position data and are pictured in Figure 20. The data are divided into the morning and afternoon shift, with the average and standard deviation of each distribution noted in the figure. In total, the two histograms represent 3,410 axle hits, and it can be concluded that both distributions follow an approximately normal distribution. These data are consistent with other wheel wander studies (Buiter et al., 1989; Timm, 1996; Stempihar et al., 2005).

When comparing the standard deviations measured at the Test Track to other studies, they are definitely on the lower end of the 8 – 24 in. scale (Buiter et al., 1989; Timm, 1996; Stempihar et al., 2005). However, when considering the limited number of vehicles and drivers, it can be concluded that the wheel wander reasonably approximates that of open-access facilities.

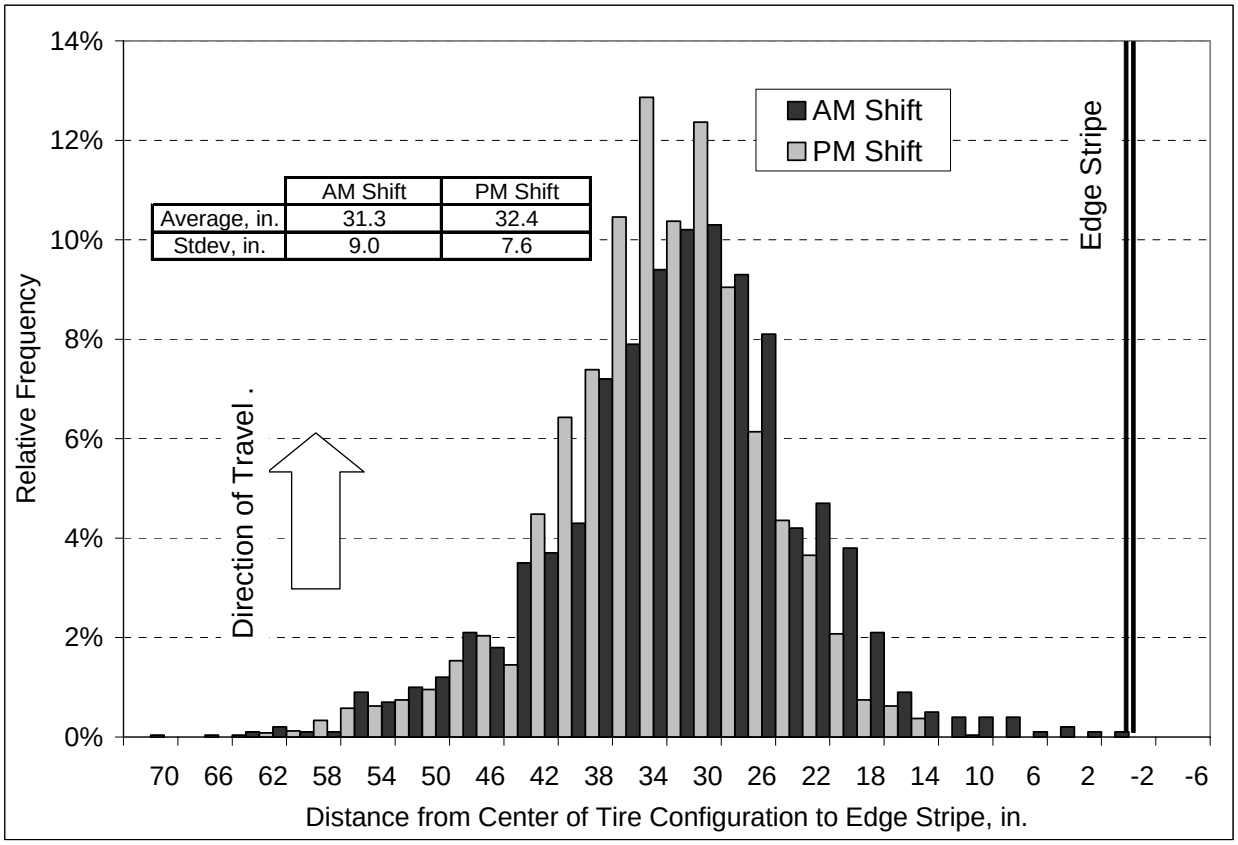

Figure 20. Statistical Summary of Wheel Wander Data.

It should be noted that there was a statistical difference between the morning and afternoon wheel wander data. A two-tailed z-test was conducted with a null hypothesis that the means of the two distributions were equal, with α equaling 0.05. The calculated z-statistic was 3.11 while the critical z-value was 1.96, resulting in rejection of the null. However, when examining the distributions in Figure 20, one could conclude that there was very little *practical* difference between the morning and afternoon data. The difference between the two means was 1.1 in., which when considered in relation to the overall lane and tire widths, is relatively small. The reason for the statistical difference was the large sample size and the fact that the z-statistic becomes larger as the sample size increases as shown by the equation:

$$z = \frac{\bar{x} - \bar{y}}{\sqrt{\frac{\sigma_1^2}{m} + \frac{\sigma_2^2}{n}}} \tag{6}$$

where: z = test statistic
$\bar{x}$ = expected value of first distribution
$\bar{y}$ = expected value of second distribution
σ_1 = standard deviation of first distribution
σ_2 = standard deviation of second distribution
m = sample size of first distribution
n = sample size of second distribution

Wheel Wander by Truck and Axle

The data summarized in Figure 20 were further divided by truck and axle number. Figures 21 and 22 indicate the average offset from the edge stripe and the variability of the wheel placement around the average, for each axle on each truck in the morning and afternoon shifts, respectively. For example, according to Figure 21, the average offset of the steer axle on Truck 1 is approximately 24 inches with about 95% (two standard deviations) of the passes within 20 inches of the average. The figures also indicate the strain gauge offsets relative to the edge stripe, with the majority of the average offsets falling between the right and center-of-wheelpath gauges. Trucks 1, 2, 3 and 4 consist of the triple trailers (Figure 2a), while Truck 5 is the box trailer (Figure 2b).

Figures 21 and 22 indicate that the placement of the steer axle is consistent between the drivers, ranging between 20 and 30 inches. However, what does vary greatly is the tracking of the trailing axles on each vehicle. For example, the trailing axles on Truck 3 gradually track further from the edge stripe. Conversely, the single axles on Truck 4 track closer to the edge stripe along the length of the trailer train. This behavior can be viewed qualitatively by inspecting Figure 23 (a) and (b) pertaining to Trucks 3 and 4, respectively. The shadows cast by the tires relative to the edge stripe clearly show the differences in alignment between the two vehicles. This has important ramifications when considering the strain measurements which will be discussed further below. It must also be noted that regardless of the driver, the trailer trains tend to track similarly between the morning and afternoon shifts. This is logical since the tracking of the trailing axles is primarily a function of the trailer alignment rather than driver-induced. Finally, it is important to note that the axles tend to pass within the transverse spread of the gauge array indicating the preliminary estimates of the outside wheelpath were accurate. These estimates were based upon the transverse location of the maximum measured rut depth from the previous research cycle at the Test Track (Timm et al., 2004).

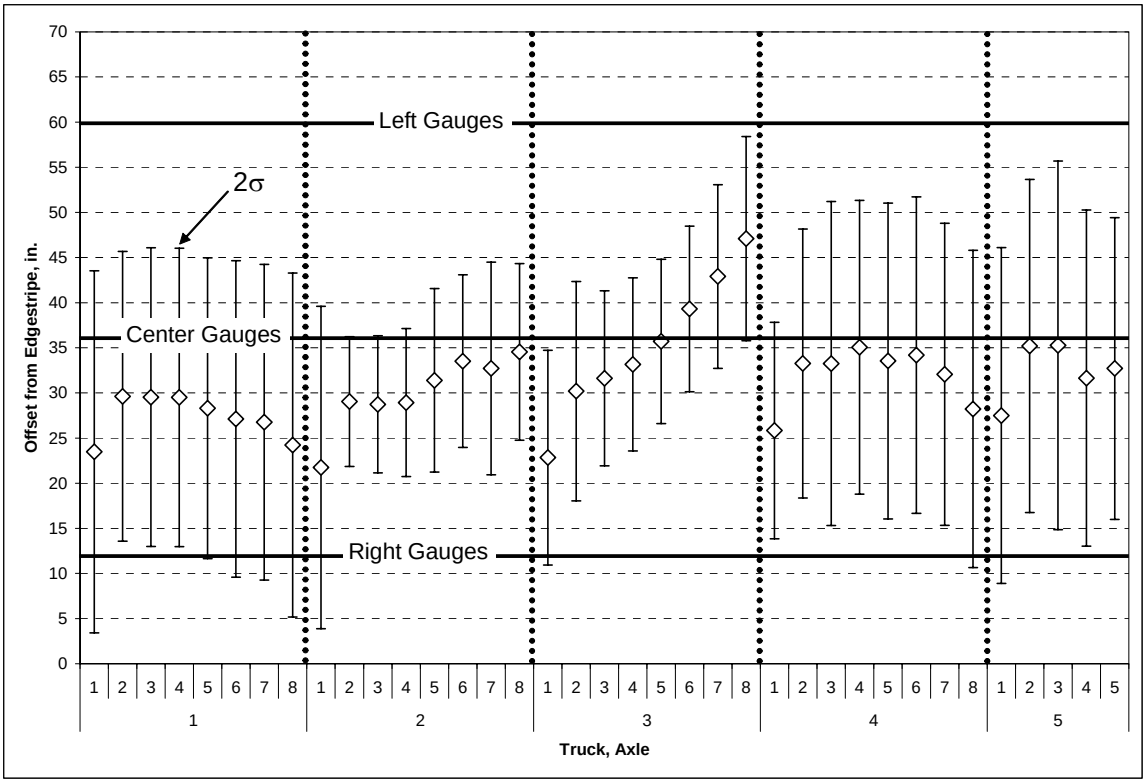

Figure 21. Wheel Wander – AM Shift.

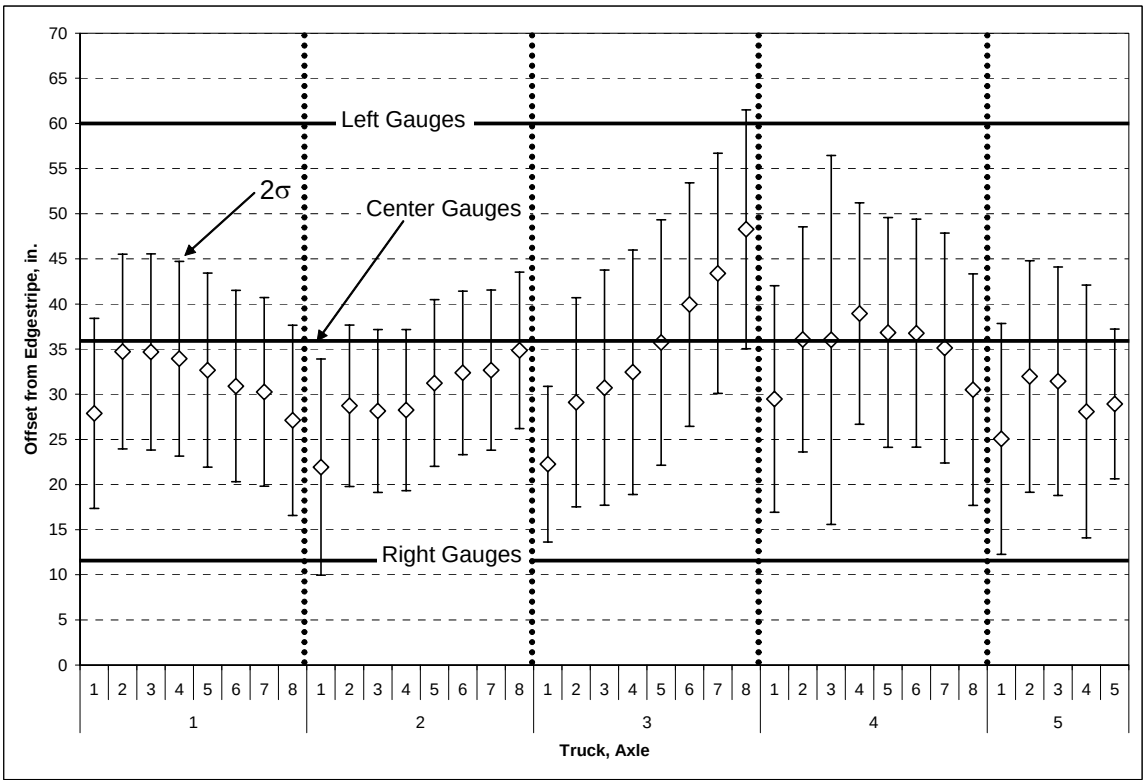

Figure 22. Wheel Wander - PM Shift.

a) Truck 3 **b) Truck 4**

Figure 23. Wheel Tracking of Single Axles.

Effect of Wheel Wander on Measured Strain

It has been observed that despite having single axles weighing the same (20 kip per axle), the measured strain tends to increase or decrease through a given truck pass as demonstrated in Figure 24. The figure shows three strain traces from gauges oriented with traffic at each lateral offset, with a line connecting the peaks of the trailing single axles (axles 4 through 8). The measured strain from the right gauge clearly decreases with each axle; the center gauge reading increases with each single axle, while the left gauge increases only slightly. For a frame of reference, the dynamic gauge array is pictured in Figure 25.

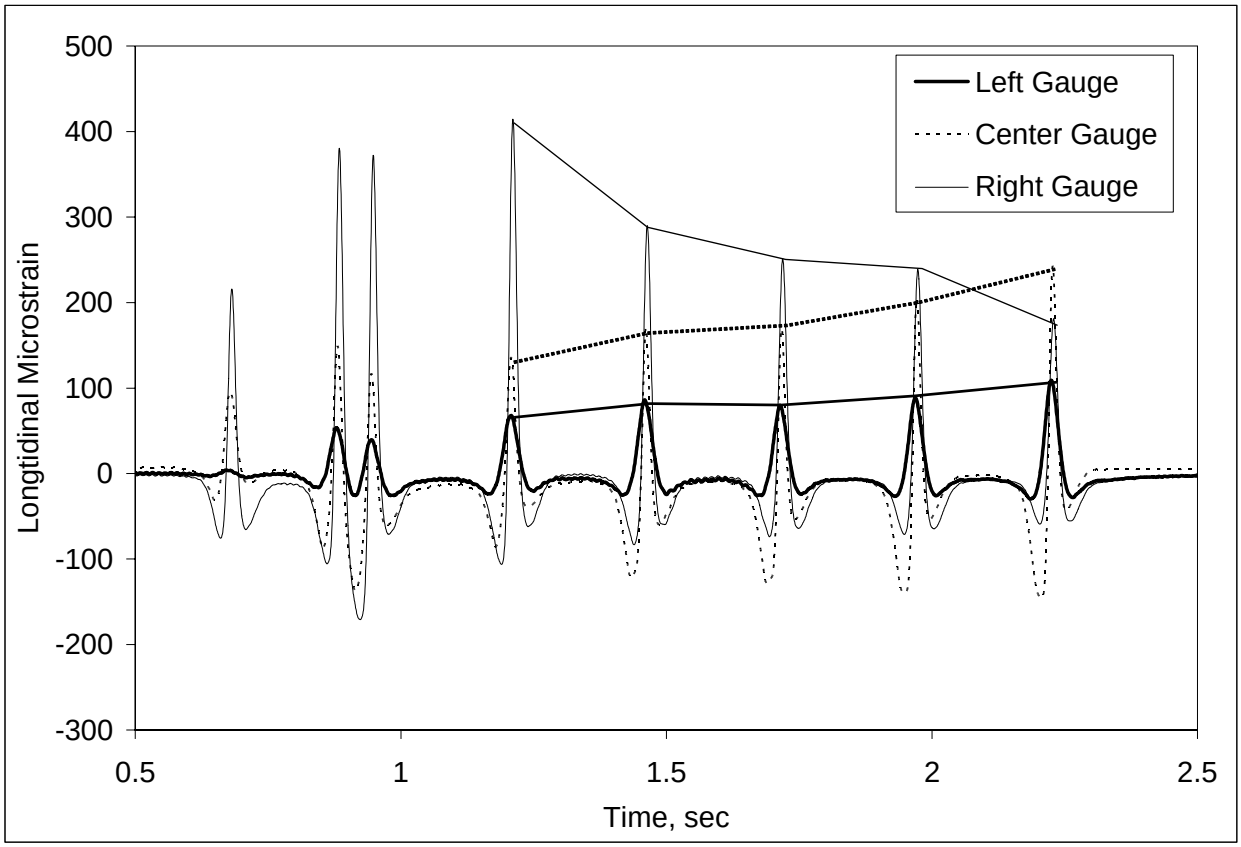

Figure 24. Dynamic Strain Traces.

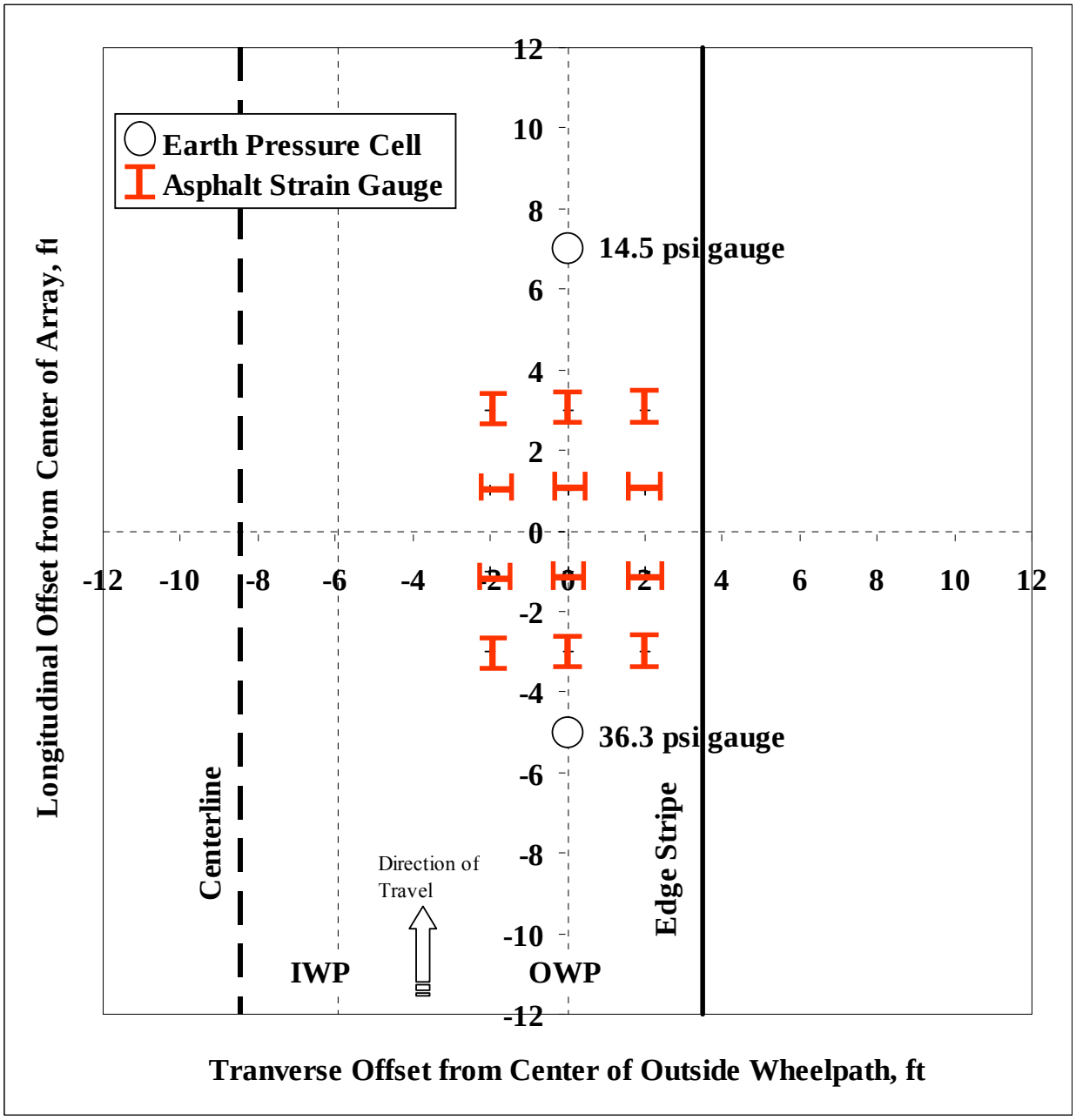

Figure 25. Dynamic Gauge Array.

While the effect of wheel wander on measured strain response is evident from a qualitative perspective in Figure 24, there is a need to quantify this effect to fully understand and assess the relationship. To facilitate this, dynamic strain data collected on July 13, 2004 in section N8 were plotted against the measured average offset using the lateral positioning system. Though approximately 800 ft from the lateral positioning system, section N8 was selected since it had the highest number of functioning gauges and could provide multiple readings at each offset (left, center and right). Also, it was hypothesized that the wheel wander near the lateral positioning system is representative of the other structural experiment test sections.

Dynamic strain measurements were obtained for three passes of Trucks 1 – 4 during the morning shift. The trailing single axles (axles 4 – 8) were used in the analysis to isolate the effect of strain versus offset since they each weigh 20 kip. The average strain per axle and per gauge were determined over the three passes. Then the average distance between the gauge and wheel load was determined from the known gauge location and measured average offset from Figure 21.

Figures 26–29 illustrate the strain vs. distance relationships for each truck, respectively. Except for Truck 3 (Figure 28), there is a strong relationship (high R^2) between strain and distance. The reason for Truck 3 as an exception is not immediately clear. However, one possibility is that the offset for Truck 3 is not as similar between the lateral positioning system and section N8 when compared to the other trucks. A portable system capable of measuring wheel wander at multiple locations would answer this question. Despite this, the graphs do show that the differences in strain response are truly a function of wheel placement. Additionally, estimates of the maximum strain from a direct hit (zero offset) can be made using the regression equations. Recall from Figure 5 that the theoretical relationship between strain and offset was approximated by a second-order polynomial, as is the case in the measured responses. This serves as a preliminary validation of layered elastic theory, however a more thorough investigation is warranted using all the test sections, strain response and backcalculated material properties which is outside the scope of this report. It must also be recognized that the second-order polynomial should only be used over the limited offsets examined in this study since it would predict higher pavement responses as the distance from the load increased beyond those presented in the figures.

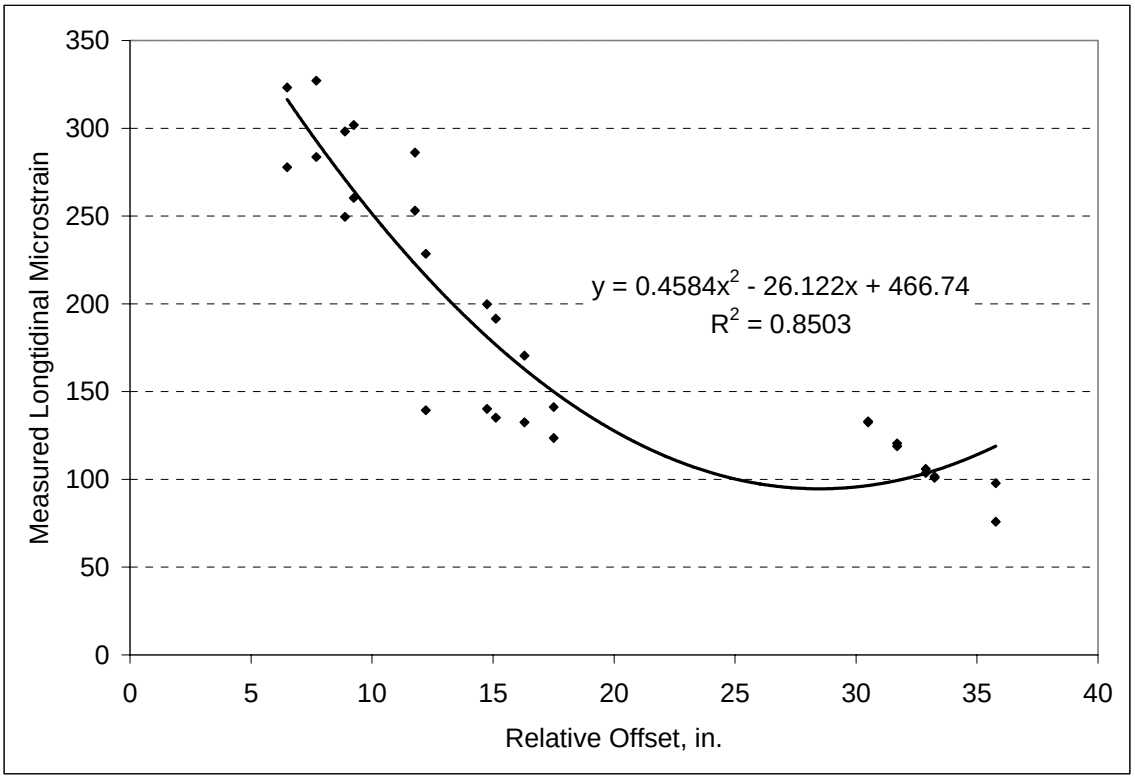

Figure 26. Strain Versus Offset – Truck 1.

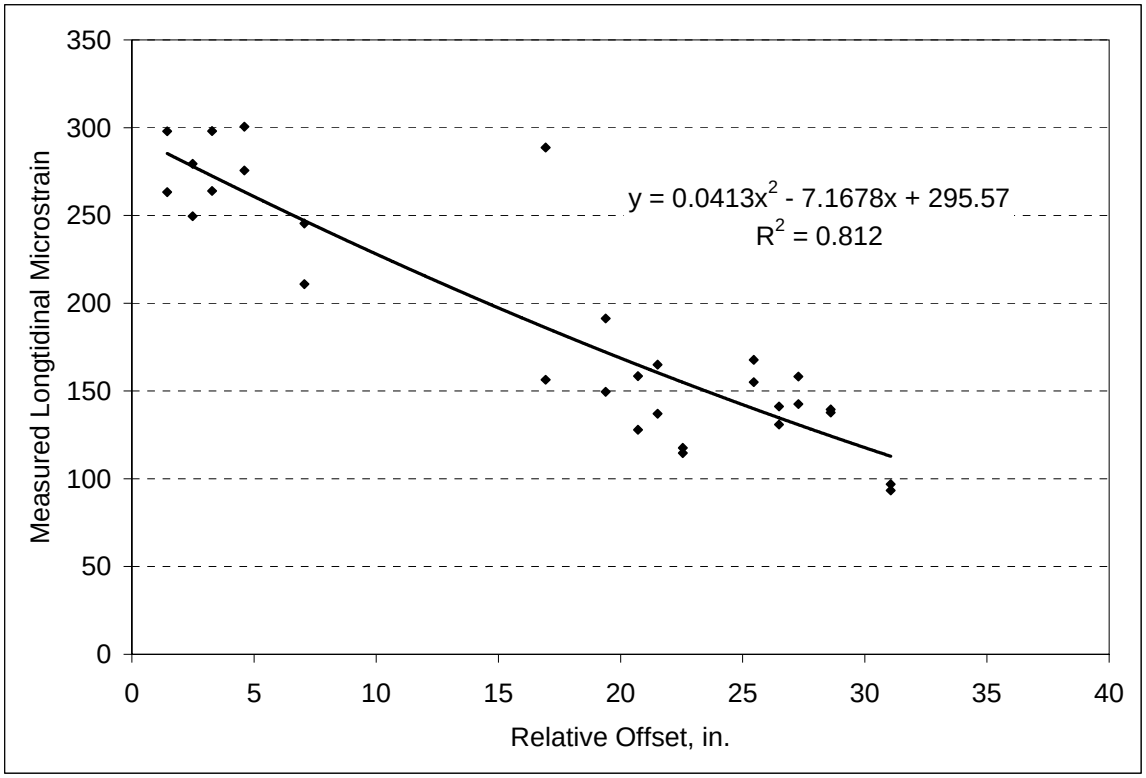

Figure 27. Strain Versus Offset – Truck 2.

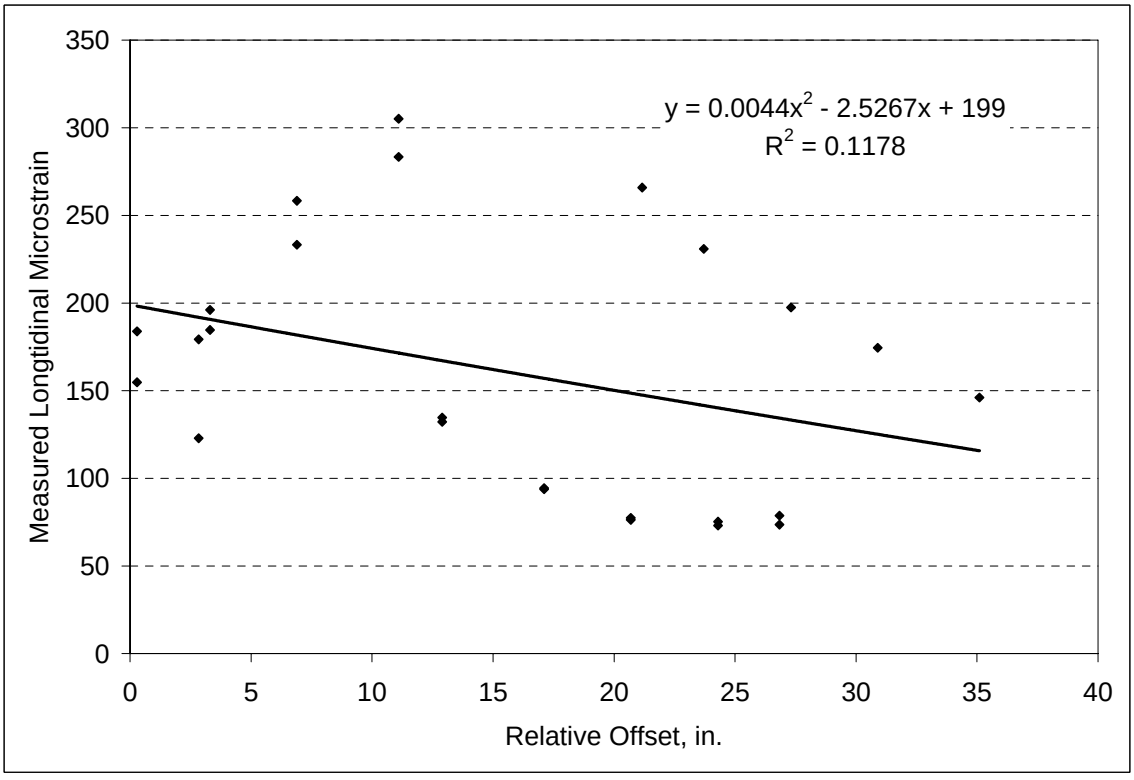

Figure 28. Strain Versus Offset – Truck 3.

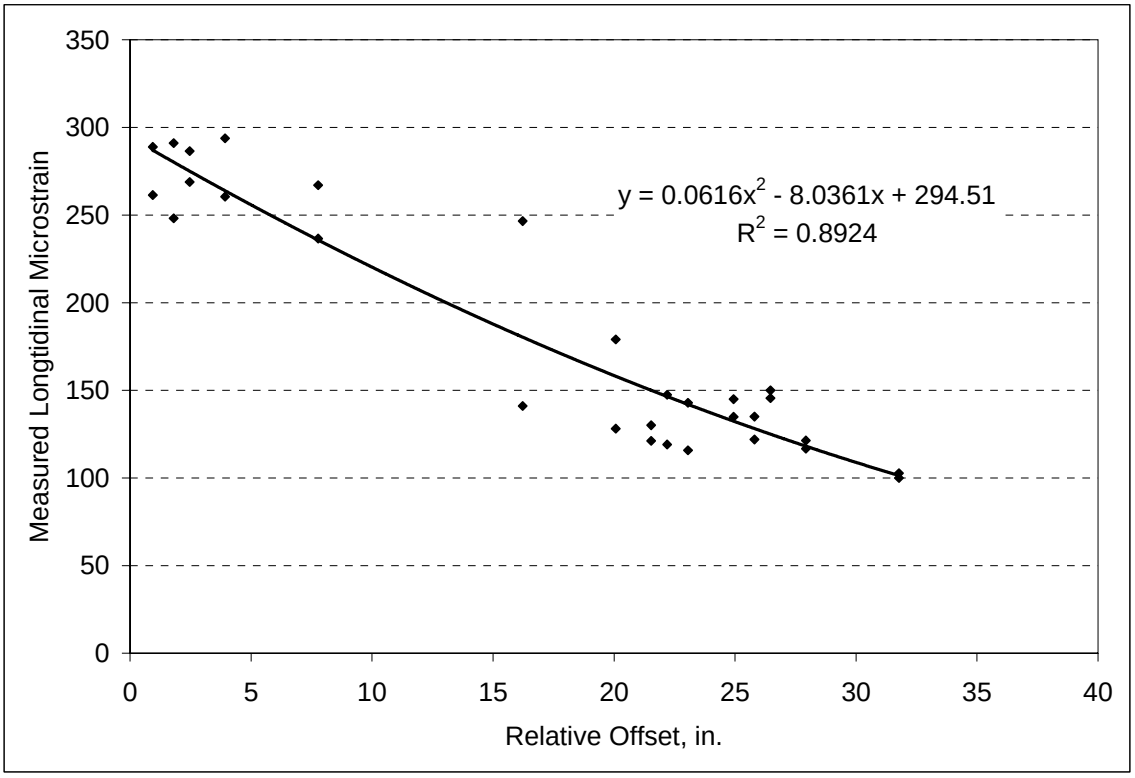

Figure 29. Strain Versus Offset – Truck 4.

CONCLUSIONS AND RECOMMENDATIONS

Wheel wander is an important parameter to measure and characterize because it has a direct impact on pavement response and performance. Based on the findings of this report, the following conclusions and recommendations can be made:

1. The lateral-positioning system used at the NCAT Test Track is a simple, yet effective and accurate means of measuring lateral offset of wheel loads.
2. The disadvantage of the lateral positioning system at the NCAT Test Track is that the location is permanent. Therefore, results from the sensors must be extrapolated to other test sections. Other systems should be considered that can be moved between sections. This is especially important for the curved sections where the wheel wander is likely different and should be characterized.
3. The measured wheel wander at the Test Track is comparable to that of open-access facilities, though its variation tends to be on the lower end of the scale reported from the literature.
4. Each vehicle and driver has a unique wheel wander pattern which should be considered in data collection and processing.
5. The original placement of the strain gauges and pressure plates was accurate relative to the applied wheel loadings (i.e., wheel loads are passing primarily within the transverse spread of the array).
6. As expected, there is a strong relationship between relative offset and strain response consistent with predictions from layered elastic theory. Further investigation of the other test sections is warranted to solidify the findings regarding section N8.

REFERENCES

1. Blab, R. and J. Litzka, "Measurements of the Lateral Distribution of Heavy Vehicles and its Effects on the Design of Road Pavements," Proceedings of the International Symposium on Heavy Vehicle Weights and Dimensions, Road Transport Technology, University of Michigan, 1995, pp. 389-395.
2. Buiter, R., W.M.H. Cortenraad, A.C. Van Eck and H. Van Rij, "Effects of Transverse Distribution of Heavy Vehicles on Thickness Design of Full-Depth Asphalt Pavements," *Transportation Research Record No. 1227*, Transportation Research Board, Washington D.C., 1989, pp. 66 – 74.
3. Epps, J.A., A. Hand, S. Seeds, T. Schulz, S. Alavi, C. Ashmore, C.L. Monismith, J.A. Deacon, J.T. Harvey, R. Leahy, "Recommended Performance-Related Specification for Hot-Mix Asphalt Construction: Results of the Westrack Project," NCHRP Report 455, Transportation Research Board, National Research Council, 2002.
4. International Road Dynamics, "Installation Manual, General Reference, Part No. 69027701," Revision D, 2003.
5. Stempihar, J.J., R.C. Williams and T.D. Drummer, "Quantifying the Lateral Displacement of Trucks for use in Pavement Design," Transportation Research Board Preprint, Washington, D.C., 2005.
6. Timm, D.H., "Investigation of Wheel Wander Effects on ESAL Calculations," Internal Report, Department of Civil Engineering, University of Minnesota, 1996.
7. Timm, D.H., A.L. Priest and T.V. McEwen, "Design and Instrumentation of the Structural Pavement Experiment at the NCAT Test Track," Report No. 04-01, National Center for Asphalt Technology, Auburn University, 2004.

APPENDIX A

LATERAL POSITIONING TIME STAMP ALGORITHM FOR USE IN DADISP 2002

```
LPS(a,W,Low,High)
{
	/*a = current window,W = number of points to average,Low = lower threshold*/ /*High
	= Upper Threshold*/
	clear(w0);
	/*Find the length of the series in the current window*/
	N=length(a);

	/*Compute the average of the first W points*/
	Avg = mean(a, 1, W);

	/*Initialize Inflection Counter*/
	counter = 1;

	Last = 0.0;
	/*Scan all the data points and look for points below the baseline*/
	for(j=W+1; j<=N-W; j++)
	{
		if(a[j] < Low && a[j-1] > High)
		{
			if({IDXTOX(a, j)}-Last > 0.034)
			{
				if(a[j+20]<Low)
				{
				concat(curr, ravel({IDXTOX(a, j)},{a[j]}));
				Last = {IDXTOX(a, j)};
				}

			}

		}

	}
}
```